

See discussions, stats, and author profiles for this publication at: <https://www.researchgate.net/publication/230663265>

# Diffusion-Influenced Excimer Formation Kinetics

ARTICLE *in* THE JOURNAL OF CHEMICAL PHYSICS · AUGUST 1991

Impact Factor: 2.95 · DOI: 10.1063/1.461029

---

CITATIONS

21

---

READS

17

## 2 AUTHORS:



[Mario N Berberan Santos](#)

University of Lisbon

**200** PUBLICATIONS **3,373** CITATIONS

SEE PROFILE



[José M G Martinho](#)

Technical University of Lisbon

**210** PUBLICATIONS **3,305** CITATIONS

SEE PROFILE

# Diffusion-influenced excimer formation kinetics<sup>a)</sup>

M. N. Berberan-Santos and J. M. G. Martinho

*Centro de Química-Física Molecular, Instituto Superior Técnico, 1096 Lisboa Codex, Portugal*

(Received 16 March 1990; accepted 15 April 1991)

A model for reversible monomer–excimer kinetics is developed, taking into account that different distributions of monomers around the excited ones are created by light absorption and excimer dissociation. The excimer formation rate coefficient departs from the Collins–Kimball equation owing to reversibility, originating significant deviations to Birks' kinetics in the monomer and excimer decays. The contribution of the geminate pair created by excimer dissociation on the overall kinetics is significant for low monomer concentrations and high viscosities. Simultaneous analysis of the monomer and excimer decay curves according to the model developed should allow to extract all the relevant information concerning the excimer formation diffusion controlled process.

## I. INTRODUCTION

The appearance of a broad structureless emission in concentrated solutions of aromatic compounds was first observed for pyrene by Förster and Kasper.<sup>1</sup> This emission was attributed to the formation of an excited dimer,<sup>1</sup> or excimer,<sup>2</sup> on the encounter of a monomer in its first excited singlet state with other monomer in the ground state. Ever since, the same phenomenon was observed for many other organic and inorganic compounds in the condensed and gas phases.<sup>3</sup> The mechanism for the excimer formation process was proposed by Förster and Kasper without allowance for reversibility.<sup>1(b)</sup> In latter work by Williams inclusion of reversibility was found necessary,<sup>4</sup> and the mechanism modified accordingly.<sup>4–6</sup> The kinetic equations of the mechanism were solved by Birks, Dyson and Munro<sup>6</sup> assuming that the excimer formation process is diffusion controlled with a rate constant equal to the long-time limit of the Smoluchowski equation.<sup>7</sup>

Since the rate coefficient for diffusion controlled processes was obtained by Smoluchowski<sup>8</sup> for the case of noninteracting spherical particles diffusing in a continuous medium, many theoretical studies appeared, clarifying and extending Smoluchowski's pioneer results.<sup>9</sup> In particular, it is found that the rate coefficient is time-dependent owing to a non-steady-state distribution of reacting molecules at early times. This was directly confirmed by time-resolved fluorescence quenching measurements.<sup>10</sup>

Monomer–excimer kinetics are generally studied using time-independent rate coefficients (Birks' kinetics<sup>6</sup>). Nevertheless, the excimer formation step is diffusion controlled and a time-dependent rate coefficient should be used. This was experimentally established for both excimer<sup>11,12(a)</sup> and exciplex<sup>12(b)</sup> kinetics in solution. Although different approaches were used to analyze the decay data, all these studies assumed that the excimer/exciplex formation rate coefficient is given by the Smoluchowski equation. For reversible systems, this is clearly a poor approximation, as “transient

effects” are repeatedly reoccurring. Several authors<sup>13–15</sup> have recently addressed the theory of reversible diffusion-influenced bimolecular reactions. Lee and Karplus<sup>13</sup> used a formalism based on a hierarchy of phenomenological kinetic equations for the reduced distribution functions of the reactant molecules and Agmon and Szabo<sup>14</sup> use modified boundary conditions in the evaluation of the survival probabilities to introduce reversibility. The particular case of monomer–excimer kinetics was addressed by André, Baros, and Winnik<sup>15</sup> following the principle of superposition of configurations.

Here, a model that considers the successive generations of monomers and excimers created at different times due to the consecutive processes of excimer dissociation and formation is used to obtain the excimer formation rate coefficient. The model also accounts for the fact that excited monomers created via light absorption and excimer dissociation have different distributions of ground-state monomers, this being mainly due to the pair of monomers (excited plus unexcited) created by excimer dissociation. The geminate pair contribution is significant for low monomer concentrations and high viscosities when excimer reversibility is considerable. It is found that the excimer formation rate coefficient depends on monomer concentration, monomer and excimer lifetimes and excimer dissociation rate constant, the Smoluchowski (or Collins–Kimball) expression being recovered only when the dissociation step is negligible. The model allows simple relationships between the excimer and monomer decay curves that can be useful in the analysis of the experimental results in contrast with previous approaches.<sup>13–15</sup> In particular, the contribution of the geminate pair to the excimer formation rate coefficient can be calculated.

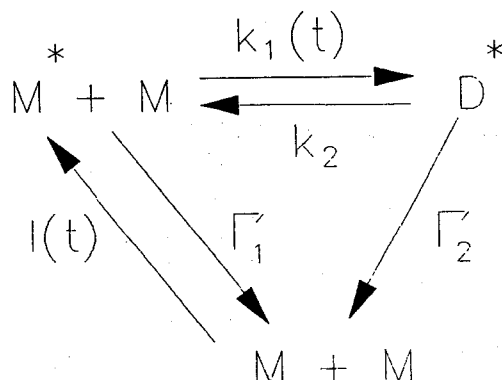
In Sec. II the model is presented and both the excimer formation rate coefficient and the monomer and excimer concentrations time evolutions are explicitly obtained considering both identical and distinct distributions of monomers around the excited ones created by light absorption and excimer dissociation. In Sec. III numerical calculations are performed in order to study the effect of concentration, excimer reversibility, diffusion coefficient, and pair effects

<sup>a)</sup> Dedicated to Dr. J. C. Conte, 1938–1990.

on the excimer formation rate coefficient and monomer and excimer decay curves. At the end the main conclusions of the treatment proposed are summarized and a method of analysis of the experimental decay curves presented.

## II. MODEL

Consider the monomer–excimer kinetic scheme



where excited monomer ( $M^*$ ), produced at a rate  $I(t)$ , may decay at an intrinsic rate  $\Gamma_1 = 1/\tau_1$ ,  $\tau_1$  being the monomer lifetime, or may react with unexcited monomer ( $M$ ) by a usually diffusion-controlled process to yield the excimer ( $D^*$ ). This may reverse back to the excited-plus-unexcited monomers with rate constant  $k_2$  or decay at an intrinsic rate  $\Gamma_2 = 1/\tau_2$ ,  $\tau_2$  being the excimer lifetime. The forward rate coefficient  $k_1$  is in general time-dependent owing to the time evolution of the distribution of  $M$  around  $M^*$ .

For  $\delta$  production of  $M^*$ , and in the absence of reversibility, the rate coefficient  $k_1$  is given by the theory of bimolecular diffusion-controlled processes.<sup>6</sup> Neglecting hydrodynamic forces and interaction potentials the pseudofirst-order rate coefficient for molecules diffusing in a continuous medium is given by the Collins–Kimball formula<sup>16</sup>

$$k_{1\delta}(t) = [M] [a + b \exp(c^2 t) \operatorname{erfc}(ct^{1/2})], \quad (1)$$

where  $[M]$  is the monomer concentration ( $\text{mol dm}^{-3}$ ),  $\operatorname{erfc}(x)$  the complementary error function and

$$a = \frac{1}{1/\alpha_T + 1/\alpha_R}, \quad (2)$$

$$b = \frac{a\alpha_R}{\alpha_T}, \quad (3)$$

$$c = \left(1 + \frac{\alpha_R}{\alpha_T}\right) \frac{D^{1/2}}{R}, \quad (4)$$

with

$$\alpha_R = k_a, \quad (5)$$

$$\alpha_T = \frac{4\pi DN_A R}{1000}, \quad (6)$$

$D$  being the mutual diffusion coefficient of  $M$  and  $M^*$  ( $D = D_M + D_{M^*}$ ),  $R$  the encounter radius,  $N_A$  the Avogadro's number and  $k_a (M^{-1}s^{-1})$  the intrinsic rate at this distance. When  $k_a$  is very large, (or more generally, for  $ct^{1/2} \gg 1$ ), the well-known Smoluchowski equation is recovered

$$k_{1\delta} = \frac{4\pi DN_A R}{1000} \left(1 + \frac{R}{\sqrt{\pi Dt}}\right) [M]. \quad (7)$$

For a general production rate of excited monomers,  $P_1$  that continuously creates a distribution of monomers identical to that produced by the initial  $\delta$  pulse and assuming linearity, i.e., absence of interference and saturation effects,

$$[M^*] = P_1 \otimes f_1, \quad (8)$$

$f_1$  being the survival probability of the excited monomer and  $\otimes$  denoting the convolution integral. Similarly, for an excimer production rate  $P_2$  one has

$$[D^*] = P_2 \otimes f_2, \quad (9)$$

$f_2$  being the survival probability of the excimer. The survival probabilities are given by

$$f_1(t) = \exp(-\Gamma_1 t) \exp\left\{-\int_0^t k_{1\delta}(u) du\right\}, \quad (10)$$

$$f_2(t) = \exp(-\Gamma_2 t) \exp(-k_2 t). \quad (11)$$

Reversibility creates excited monomers, via excimer dissociation, at a rate  $k_2 [D^*]$ . The excited monomer production term is therefore composed by an external component  $I$ , owing to photon absorption and by an internal component  $k_2 [D^*]$ . The excimer production term is on the other hand  $P_2 = k_1 [M^*]$ , since excimers are only created in the excimer formation step. Hence,

$$P_1 = I + k_2 [D^*], \quad (12)$$

$$P_2 = k_1 [M^*]. \quad (13)$$

Assuming that the distribution of monomers around the excited one is identical for both external and internal production terms, Eqs. (8) and (9) apply, yielding

$$[M^*] = (I + k_2 [D^*]) \otimes f_1, \quad (14)$$

$$[D^*] = (k_1 [M^*]) \otimes f_2, \quad (15)$$

with<sup>17</sup>

$$k_1 = \frac{P_1 \otimes (k_{1\delta} f_1)}{P_1 \otimes f_1} = \frac{(I + k_2 [D^*]) \otimes (k_{1\delta} f_1)}{(I + k_2 [D^*]) \otimes f_1}. \quad (16)$$

This being different from  $k_{1\delta}$ .

Application of Laplace transform  $\mathcal{L}$  to Eqs. (14)–(16) allows the separation of  $[M^*]$  and  $[D^*]$ , these being obtained after Laplace inversion as

$$[M^*] = I \otimes J \otimes f_1, \quad (17)$$

$$[D^*] = I \otimes J \otimes (k_{1\delta} f_1) \otimes f_2, \quad (18)$$

$$k_1 = \frac{I \otimes J \otimes (k_{1\delta} f_1)}{I \otimes J \otimes f_1} = \frac{I \otimes J \otimes (k_{1\delta} f_1)}{[M^*]}, \quad (19)$$

where the secondary production rate  $J$  is given by

$$J = \mathcal{L}^{-1} \left[ \frac{1}{1 - \mathcal{L}[k_{1\delta} f_1] \mathcal{L}[k_2 f_2]} \right]. \quad (20)$$

The time evolutions of the monomer and the excimer, Eqs. (17) and (18), respectively, were obtained before by Sienicki and Winnik<sup>18</sup> by an iterative procedure and Vogelsang and Hauser<sup>19</sup> using the concept of convolution kinetics.

If the process of excimer formation is irreversible ( $k_2 = 0$ ), then  $J = \delta(t)$ ; otherwise it is a composite function

of  $t$ ,  $\delta(t)$  plus a bell-shaped function. The shape of the secondary production rate  $J$  is best seen by its calculation within Birks' kinetics (time-independent  $k_1 = a[M]$ ). From Eq. (20) one obtains

$$J = \delta + \frac{k_1 k_2}{\lambda_2 - \lambda_1} (e^{-\lambda_1 t} - e^{-\lambda_2 t}), \quad (21)$$

where  $\lambda_1$  and  $\lambda_2$  are the decay constants in Birks' monomer-excimer kinetics

$$\lambda_{1,2} = \frac{1}{2} \{ (A_X + A_Y) \pm \sqrt{(A_X - A_Y)^2 + 4k_1 k_2} \}, \quad (22)$$

$A_X, A_Y$  being given by

$$A_X = \Gamma_1 + k_1, \quad (23)$$

$$A_Y = \Gamma_2 + k_2. \quad (24)$$

The significance of Eq. (21) is clear: superposed to the direct production by external means (photon absorption) is a delayed term that closely parallels the excimer time evolution, resulting from excimer dissociation back to excited monomer, that creates a time lag between external and internal production contributions. These findings are not qualitatively modified upon consideration of the transient contribution. In fact using the identity

$$J \otimes (k_{1\delta} f_1) \otimes k_2 f_2 = J - \delta, \quad (25)$$

one obtains from Eq. (18) that, for  $I = \delta$ ,

$$J = \delta + k_2 [D^*] \quad (26)$$

hence a time lag between external and internal production contributions always arises.

Nevertheless, the assumption made of a uniform distribution of monomers around the excited ones created by excimer dissociation is a poor approximation at least for low monomer concentrations and high viscosities. Indeed, the contribution to the overall excimer formation rate coefficient of the pair of excited plus unexcited monomers in proximity created by excimer dissociation should be important since the other monomers are far apart and the viscosity prevents on the one hand the "dissociation" of the pair and on the other hand the approximation of the other monomers towards the excited one. The model can be extended to incorporate these effects since the rate coefficient for the distribution of monomers around the excited one created by excimer dissociation,  $k'_{1\delta}$ , is known. If all the monomers but one are randomly distributed, and that one is at the encounter distance, as is approximately the case (see Sec. IV), the rate coefficient has a simple expression given by<sup>20</sup> (Appendix A)

$$k'_{1\delta} = k_{1\delta} - \frac{d \ln k_{1\delta}}{dt}. \quad (27)$$

The first term of Eq. (27) is related to the distribution of monomers around the excimer just before dissociation while the second refers to the geminate pair of monomers (excited plus unexcited) created when the excimer dissociates. Monomer and excimer concentration time evolutions [Eqs. (14) and (15)] should be modified given the presence of both types of excited monomers, hence

$$[M^*] = I \otimes f_1 + k_2 [D^*] \otimes f'_1, \quad (28)$$

$$[D^*] = [k'_1 (I \otimes f_1)] \otimes f_2 + [k'_1 (k_2 [D^*] \otimes f'_1)] \otimes f_2, \quad (29)$$

$k'_1$  and  $k'_1$  being the rate coefficients for external and internal production of excited monomers, respectively,

$$k'_1 = \frac{I \otimes (k_{1\delta} f_1)}{I \otimes f_1}, \quad (30)$$

$$k'_1 = \frac{k_2 [D^*] \otimes (k'_{1\delta} f'_1)}{k_2 [D^*] \otimes f'_1}, \quad (31)$$

and

$$f'_1(t) = \exp(-\Gamma_1 t) \exp\left[-\int_0^t k'_{1\delta}(u) du\right], \quad (32)$$

this being the survival probability of the monomers created by excimer dissociation.

Application of Laplace transforms to Eqs. (28) and (29), now gives

$$[M^*] = I \otimes f_1 + I \otimes J' \otimes (k_{1\delta} f_1) \otimes (k_2 f_2) \otimes f'_1, \quad (33)$$

$$[D^*] = I \otimes J' \otimes (k_{1\delta} f_1) \otimes f_2, \quad (34)$$

with

$$J' = \mathcal{L}^{-1} \left[ \frac{1}{1 - \mathcal{L}[k'_{1\delta} f'_1] \mathcal{L}[k_2 f_2]} \right]. \quad (35)$$

Equations (33)–(35) are therefore a more general model for monomer-excimer kinetics.

Within the present formalism, the usual rate equations of formal kinetics

$$\frac{d[M^*]}{dt} = I + k_2 [D^*] - (\Gamma_1 + k_1) [M^*], \quad (36)$$

$$\frac{d[D^*]}{dt} = k_1 [M^*] - (\Gamma_2 + k_2) [D^*] \quad (37)$$

still hold, provided  $k_1$  is a generalized rate coefficient, given by (Appendix B)

$$k_1 = \frac{I \otimes (k_{1\delta} f_1) + I \otimes J' \otimes (k_{1\delta} f_1) \otimes (k_2 f_2) \otimes (k'_{1\delta} f'_1)}{I \otimes f_1 + I \otimes J' \otimes (k_{1\delta} f_1) \otimes (k_2 f_2) \otimes f'_1}. \quad (38)$$

Using again the identity similar to Eq. (25),  $J' \otimes (k'_{1\delta} f'_1) \otimes k_2 f_2 = J' - \delta$  one can rewrite  $k_1$  as

$$k_1 = \frac{I \otimes J' \otimes (k_{1\delta} f_1)}{[M^*]}, \quad (39)$$

which still has the form of Eq. (19). Adding Eqs. (36) and (37) one obtains

$$\frac{d}{dt} ([M^*] + [D^*]) = I - \Gamma_1 [M^*] - \Gamma_2 [D^*], \quad (40)$$

which can be written in an integral form in two alternative ways,

$$[M^*] + [D^*] = I \otimes \exp(-\Gamma_2 t) + (\Gamma_2 - \Gamma_1) [M^*] \otimes \exp(-\Gamma_2 t), \quad (41a)$$

$$[M^*] + [D^*] = I \otimes \exp(-\Gamma_1 t) + (\Gamma_1 - \Gamma_2) [D^*] \otimes \exp(-\Gamma_1 t). \quad (41b)$$

These equations relate monomer and excimer in a simple way. Note also that Eq. (37) implies a simple convolution relation between monomer and excimer,

$$[D^*] = (k_1[M^*]) \otimes f_2. \quad (42)$$

This relation resembles the one obtained in Ref. 15, but with the important difference that  $k_{1\delta}$  has been replaced by  $k_1$ . This difference remains even in the case of equivalent external and internal production terms, where  $k_1$  is given by Eq. (19). Only when the external production term is a  $\delta$  function and  $k_2 = 0$  is the rate coefficient equal to  $k_{1\delta}$ .

When the primary production rate  $I(t)$  is of  $\delta$  type, the time-dependent rate coefficient becomes

$$k_1 = \frac{(k_{1\delta}f_1) + k_2[D^*] \otimes (k'_{1\delta}f'_1)}{f_1 + k_2[D^*] \otimes f'_1}. \quad (43)$$

It can be anticipated from this relation that a limit value,  $k_1(\infty)$ , will be obtained for sufficiently long times.

It is of interest to put bounds on  $k_1(\infty)$ . The lower bound is attained for irreversibility conditions ( $k_2 = 0$ ),

$$k_1(\infty) = \lim_{t \rightarrow \infty} k_{1\delta}(t) = a[M]. \quad (44)$$

On the other hand, when  $k_2$  is very large,  $[D^*]$  rises very fast, and then decays at a slower rate. If this decay is sufficiently slow so that  $[D^*]$  is approximately constant on a sufficient time scale,

$$k_1^{ss} = \lim_{t \rightarrow \infty} \frac{I_0 \otimes (k_{1\delta}f_1) + I_0 \otimes J' \otimes (k_{1\delta}f_1) \otimes (k_2f_2) \otimes (k'_{1\delta}f'_1)}{I_0 \otimes f_1 + I_0 \otimes J' \otimes (k_{1\delta}f_1) \otimes (k_2f_2) \otimes f'_1}. \quad (49)$$

Note that owing to the concentration dependence of  $k_1^{ss}$ ,  $h$  is also concentration-dependent. The corresponding equation for equivalent external and internal production of excited monomers is recovered for  $k'_{1\delta} = k_{1\delta}$ .

### III. NUMERICAL RESULTS

Monomer and excimer decays, as well as the forward rate coefficient  $k_1$ , are now numerically computed for several realistic cases, assuming a  $\delta$  pulse as the external production rate. The results obtained according to the convolution model for both equivalent and nonequivalent modes of external and internal excited monomer production are compared with those obeying Birks' kinetics.

The monomer and excimer decay curves for nonequivalent excited monomer production modes were calculated from Eqs. (33) and (34) with  $I = \delta$ , and the counterpart equations for equivalent production modes from Eqs. (17) and (18). The secondary production rates  $J$  [Eq. (20)] and  $J'$  [Eq. (35)] were evaluated by numerical inversion of the Laplace transform (Appendix C). The forward rate coefficient was calculated for both equivalent [Eq. (19)] and nonequivalent [Eq. (39)] excited monomer production modes after knowing  $[M^*]$ .

The decay curves and rate coefficient  $k_1$  were evaluated using monomer and excimer lifetimes, respectively, of 10

$$k_1(\infty) = \langle k_{1\delta} \rangle = \int_0^\infty k'_{1\delta}(t)f'_1(t)dt / \int_0^\infty f'_1(t)dt, \quad (45)$$

hence the decay-weighted rate coefficient  $k_{1\delta}$  is obtained, as occurs in an irreversible system for the photostationary state.

Whenever  $k_1(\infty)$  is attained very fast compared to the time scale of the overall decay, Birks' kinetics (time-independent rate coefficients) become approximately valid as the rate coefficient  $k_1$  is time-independent. In such a case, therefore, Birks behavior is expected, but with a rate constant  $k_1$  given by  $k_1(\infty)$  and not by  $\lim_{t \rightarrow \infty} k_{1\delta}(t)$ .

The photostationary state, i.e., the limit of large time when the primary production rate is constant,  $I(t) = I_0$ , is obtained from Eqs. (36) and (37) as

$$[M^*]_{ss} = \frac{I_0}{\Gamma_1(1 + 1/h)}, \quad (46)$$

$$[D^*]_{ss} = \frac{I_0}{\Gamma_2(1 + h)}, \quad (47)$$

$h$  being given by

$$h = \frac{\Gamma_1(k_2 + \Gamma_2)}{\Gamma_2 k_1^{ss}}, \quad (48)$$

which is a generalization of the analogous equations in Birks' kinetics,<sup>3</sup> with the rate constant  $k_1^{ss}$  given by

and 20 ns, monomer concentrations varying between  $10^{-2}$  and 1 M and within each concentration for various degrees of reversibility, the backward rate constant  $k_2$  taking values between 0 and  $10^8 \text{ s}^{-1}$ . The rate coefficient  $k_{1\delta}$  was calculated by the Collins-Kimball expression [Eq. (1)] with  $D = 10^{-5} \text{ cm}^2 \text{ s}^{-1}$  or  $D = 10^{-6} \text{ cm}^2 \text{ s}^{-1}$ ,  $R = 8 \text{ \AA}$  and the intrinsic rate constant  $k_a = 10^{10} \text{ M}^{-1} \text{ s}^{-1}$ .

Figure 1 shows the time evolution of the forward rate coefficient  $k_1$ , calculated for  $[M] = 0.1 \text{ M}$  and  $D = 10^{-5} \text{ cm}^2 \text{ s}^{-1}$  for  $k_2 = 10^7 \text{ s}^{-1}$  and  $k_2 = 10^8 \text{ s}^{-1}$  taking and not taking into account pair effects.

For short times  $k_1$  decreases with time as  $k_{1\delta}$ , since at early times only the excited monomers created by photon absorption are important. With the passage of time reversibility creates a new kind of excited monomers that decay with a higher rate coefficient ( $k'_{1\delta}$ ) leading to a progressive increase of the overall rate coefficient. This growth is the more important the higher  $k_2$  this being especially notorious when pair effects are considered. The depart of  $k_1$  occurs early for larger  $k_2$ , attaining for long times a near constant value. The contribution of the geminate pair recombination is significant for both  $k_2$  values, the rate of growth being slower for the smaller backward rate constant  $k_2$ . For  $k_2 = 10^6 \text{ s}^{-1}$  reversibility is unimportant and the rate coefficient  $k_1$  is near  $k_{1\delta}$  over the time range of interest. This explains why a good

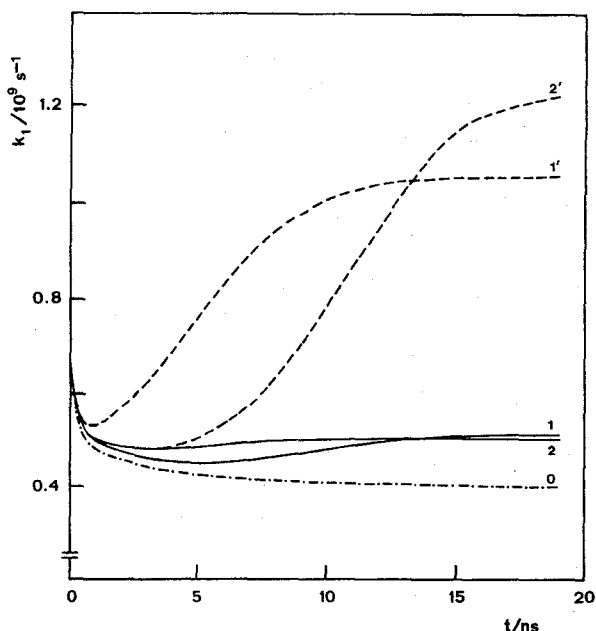


FIG. 1. Excimer formation rate coefficient vs time with  $D = 10^{-5} \text{ cm}^2 \text{ s}^{-1}$ ,  $[M] = 0.1 \text{ M}$  and  $k_2 = 10^8 \text{ s}^{-1}$  (1,1'),  $k_2 = 10^7 \text{ s}^{-1}$  (2,2'). The curves labeled without a prime were calculated from Eq. (19) (without pair effects) and with a prime from Eq. (39), considering the geminate pair contribution. (0) Collins-Kimball rate coefficient calculated from Eq. (1).

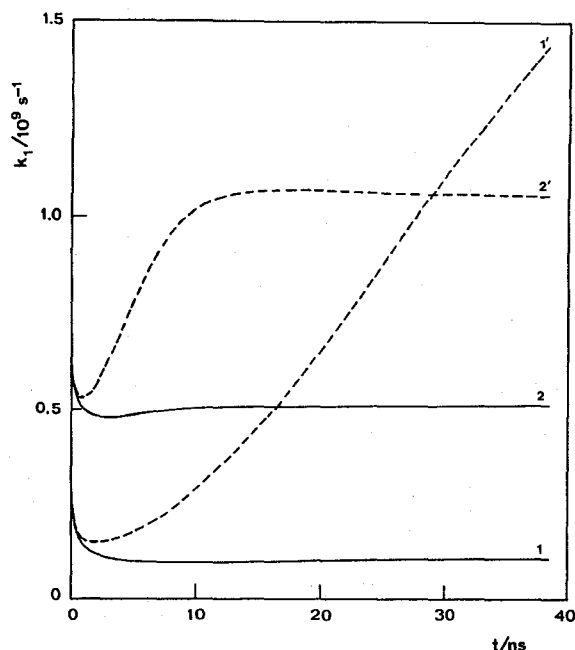


FIG. 2. Excimer formation rate coefficient vs time with  $k_2 = 10^8 \text{ s}^{-1}$ ,  $[M] = 0.1 \text{ M}$ , and  $D = 10^{-6} \text{ cm}^2 \text{ s}^{-1}$  (1,1'),  $D = 10^{-5} \text{ cm}^2 \text{ s}^{-1}$  (2,2'). The curves labeled without a prime were calculated from Eq. (19) (without pair effects) and with a prime from Eq. (39), considering the geminate pair contribution.

fit was obtained for the simultaneous analysis of the excimer and monomer decay curves of pyrene solutions,<sup>11</sup> near room temperature ( $k_2 \sim 10^6 \text{ s}^{-1}$ ) using the convolution relation 42 with  $k_1 = k_{1\delta}$ , which allows the evaluation of  $D$  and  $R$  of the Smoluchowski's equation. Nevertheless, the use of the Smoluchowski rate coefficient is always an approximation, and not an exact result. In order to see the influence of the diffusion coefficient we plot on Fig. 2  $k_1$  for  $D = 10^{-5} \text{ cm}^2 \text{ s}^{-1}$  and  $D = 10^{-6} \text{ cm}^2 \text{ s}^{-1}$  maintaining the monomer concentration equal to  $[M] = 0.1 \text{ M}$ , and  $k_2 = 10^8 \text{ s}^{-1}$ . Comparison of the set of curves with and without pair effects for both diffusion coefficients clearly show the increasing importance (for long times) of the geminate pair recombination contribution with the decrease of  $D$ .

This is understandable since the decrease of  $D$  on one hand makes pair separation difficult and on the other hand prevents the approximation of the other monomers towards the excited one. The growing of  $k_1$  with time is slower for  $D = 10^{-6} \text{ cm}^2 \text{ s}^{-1}$ , essentially due to the shape of the excimer decay [see Eq. (43)]. Indeed after the minimum,  $k_1$  increases with the rise of the excimer attaining a quasistationary value when the excimer decay can be considered nearly constant [see Eq. (45)]. As the rise time of the excimer decreases with an increase of  $D$ , the rate of growth of  $k_1$  is lower for the lower diffusion coefficient. In order to see the influence of monomer concentration the rate coefficient  $k_1$  was plotted in Fig. 3 maintaining  $D = 10^{-6} \text{ cm}^2 \text{ s}^{-1}$  and  $k_2 = 10^8 \text{ s}^{-1}$  for  $[M] = 10^{-2} \text{ M}$ ,  $[M] = 10^{-1} \text{ M}$ , and  $[M] = 1 \text{ M}$ .

The higher the monomer concentration the smaller are the differences between the curves calculated with and with-

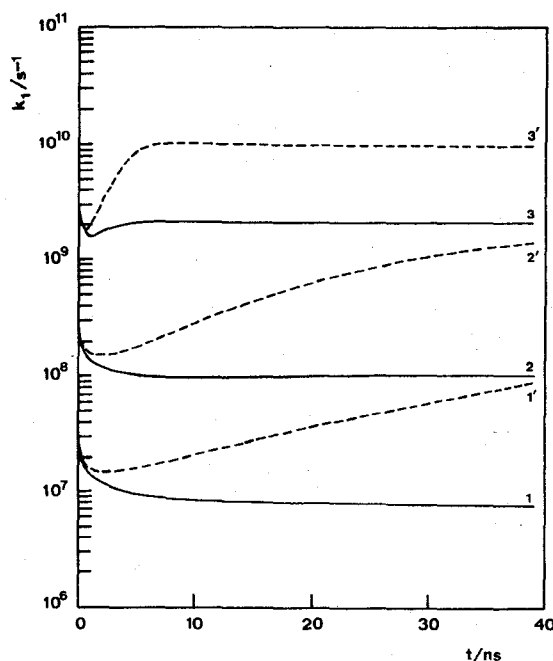


FIG. 3. Excimer formation rate coefficient vs time with  $k_2 = 10^8 \text{ s}^{-1}$ ,  $D = 10^{-6} \text{ cm}^2 \text{ s}^{-1}$  and  $[M] = 0.01 \text{ M}$  (1,1'),  $[M] = 0.1 \text{ M}$  (2,2'),  $[M] = 1 \text{ M}$  (3,3'). The curves labeled without a prime were calculated from Eq. (19) (without pair effects) and with a prime from Eq. (39), considering the geminate pair contribution.

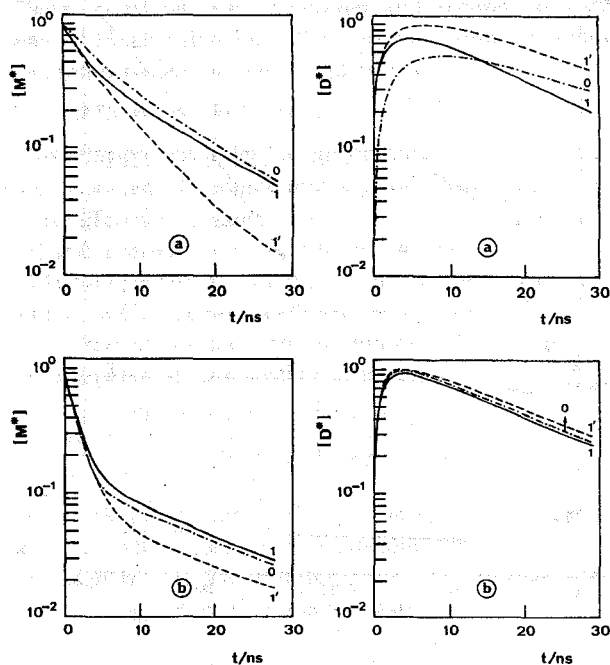


FIG. 4. Monomer and excimer decay curves with  $[M] = 0.1 \text{ M}$ ,  $k_2 = 10^8 \text{ s}^{-1}$  and  $D = 10^{-6} \text{ cm}^2 \text{ s}^{-1}$  (a),  $D = 10^{-5} \text{ cm}^2 \text{ s}^{-1}$  (b). (0) According to Birks' model; (1) from Eqs. (17) and (18) (without pair effects); (1') from Eqs. (33) and (34) considering the geminate pair contribution. Excimer decay curves are normalized with respect to the maximum of the highest one in each figure.

out pair effects. This is expected since at higher monomer concentrations, the uniform background concentration should prevail over the comparatively small change due to pair formation/dissociation, and  $k'_{1\delta}$  approximates  $k_{1\delta}$ . Nevertheless, differences are still significant for the highest concentration considered, 1 M. The time evolution of the forward rate coefficient for sufficiently high values of  $[M]$  and/or  $k_2$  shows a minimum for short times and attain very quickly a near constant value for longer times. This minimum is shifted towards smaller times with the increase on concentration, occurring in the subnanosecond or even picosecond time region for high enough concentrations. In this case approximate Birks' behavior is expected with a rate constant  $k_1$  differing from  $\lim_{t \rightarrow \infty} k_{1\delta}$ . Similar results were obtained by André, Baros, and Winnik<sup>15</sup> using the principle of superposition of configurations. However, these authors were not able to obtain analytical expressions for the decay curves and rate coefficient, which limitates the applicability of their model.

Monomer and excimer profiles are shown in Figs. 4 and 5 together with the results from Birks' kinetics with  $k_1 = \lim_{t \rightarrow \infty} k_{1\delta} = a[M]$ .

From the above results it is seen that deviations to Birks' kinetics are the rule with the present model. These are clearly shown on the excimer decay curves, that owing to the transient contribution of the excimer formation rate coefficients have shorter rise times than Birks' kinetics predict. The set of Figs. 4(a)–4(d) show for a monomer concentra-

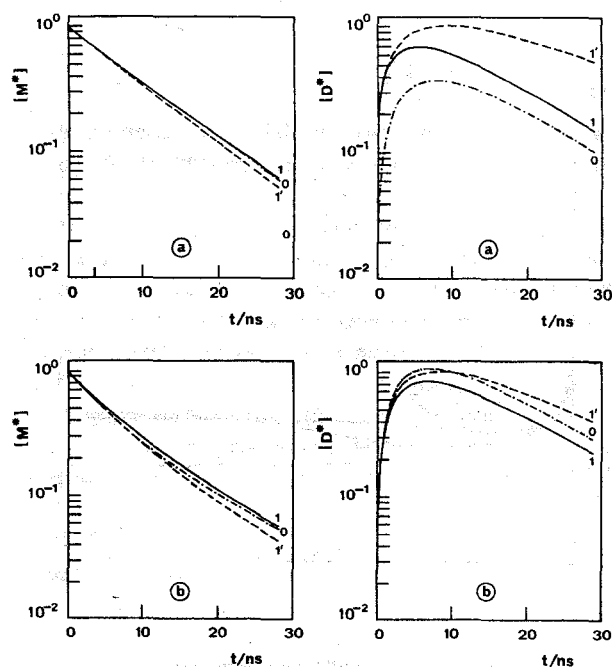


FIG. 5. Monomer and excimer decay curves with  $[M] = 0.01 \text{ M}$ ,  $k_2 = 10^8 \text{ s}^{-1}$  and  $D = 10^{-6} \text{ cm}^2 \text{ s}^{-1}$  (a),  $D = 10^{-5} \text{ cm}^2 \text{ s}^{-1}$  (b). (0) According to Birks' model; (1) from Eqs. (17) and (18) (without pair effects); (1') from Eqs. (33) and (34) considering the geminate pair contribution. Excimer decay curves are normalized with respect to the maximum of the highest one in each figure.

tion of  $10^{-1} \text{ M}$  and  $k_2 = 10^8 \text{ s}^{-1}$  the influence of the diffusion coefficient ( $D = 10^{-6} \text{ cm}^2 \text{ s}^{-1}$ ,  $D = 10^{-5} \text{ cm}^2 \text{ s}^{-1}$ ) on both monomer and excimer decay curves. The decay curves show that the geminate pair contribution is higher for the lower diffusion coefficient, this being particularly clear in the excimer decays. In Figs. 5(a)–5(d) is also shown the influence of  $D$  on both monomer and excimer decay curves but now for a concentration of  $10^{-2} \text{ M}$ . The decay curves show similar trends as observed in Fig. 4. Comparison of the set of excimer decay curves in Figs. 4 and 5 indicates that the geminate pair contribution is higher for the lower concentration, the opposite being observed for the monomer decay. Although it is true that the contribution of the geminate pair to  $k'_{1\delta}$  increase with the decrease of concentration the same need not be observed with  $k_1$ . Indeed,  $k_1$  depends not only on  $k_{1\delta}$  but also on the amount of delayed excimer, which increases with concentration. Therefore to explain the concentration dependence of the pair effect, these two effects, which work in opposition, must be considered. The same kind of reasoning is applicable to the variations of  $k_1$  with  $k_2$  or  $D$ , since both parameters influence the degree of reversibility.

The shape of the decay curves show that a careful analysis of the experimental curves should provide quantitative information on both the time dependence of the forward rate coefficient and on the contribution of the geminate pair of monomers.

#### IV. SUMMARY AND CONCLUSIONS

A model for reversible monomer–excimer kinetics is formulated under the assumption of linearity for the production of excited species. This is reasonable for the low intensities of excitation light commonly employed. In such circumstances, excited species are, on the average, very far apart, and interference and saturation effects are negligible for phenomena occurring in the nano or subnanosecond time scale. It is also assumed that light absorption creates excited monomers with an uniform distribution of ground state monomers and that excimer dissociation creates a ground state monomer distribution that can be described as a superposition of an uniform distribution plus a pair of monomers (excited plus unexcited) in contact. While excitation via light absorption is a spatially random process and therefore corresponds to an essentially uniform radial distribution function of ground state monomers around the excited ones, excited monomer production via excimer dissociation can deviate from the assumed superposition of configurations. Indeed, the distribution of ground state monomers around the excimer just before excimer dissociation may not be uniform since excimers are created from excited monomers with distributions that are not uniform. Molecular diffusion tends to reestablish a uniform distribution of monomers around the excimer. However, this effect is dependent on the rate of excimer dissociation: For very fast dissociation it is negligible and the average distribution of ground state monomers around the excited monomer is close to the one that originated the excimer. Conversely, for slow excimer dissociation, a close to uniform distribution around the excimer can be attained before dissociation occurs.

Reversibility is shown to have the effect of making the forward (excimer formation) rate coefficient depart from the Collins–Kimball (Smoluchowski) expression. The monomer and excimer decay curves show significant deviations to Birks' kinetics, which are more visible in the rise portion of the excimer decay. The consideration of the geminate pair recombination contribution influences the decay curves and the forward rate coefficient,  $k_1$ , this effect being more pronounced for low monomer concentrations and high viscosities. The expressions of the monomer and excimer decay curves and forward rate coefficient are very complex, which makes the analysis of the experimental results difficult. However, from the simultaneous analysis of the excimer and monomer decay curves following Eqs. 41(a) and 41(b) the reciprocal lifetime  $\Gamma_2$  can be evaluated ( $\Gamma_1$  is known for measurements with diluted solutions). On the other hand, the diffusion coefficient  $D$ , the encounter radius  $R$ , the intrinsic rate constant  $k_a$  of the Collins–Kimball expression, and  $k_2$  can be evaluated from the simultaneous analysis of monomer and excimer decay curves following Eq. (28). This relation also allows the estimation of the geminate pair recombination contribution that is apparent in  $f'_1$ . Indeed, when the geminate pair recombination contribution is negligible  $f'_1 = f_1$  and Eq. (28) reduces to Eq. (14).

#### ACKNOWLEDGMENTS

This work was supported by JNICT (Junta Nacional de Investigação Científica e Tecnológica) project

PMCT/C/CEN/333/90 and by INIC (Instituto Nacional de Investigação Científica). The authors acknowledge J. P. Pinheiro and J. P. Farinha for performing the numerical calculations.

#### APPENDIX A: DERIVATION OF THE ASSOCIATION RATE COEFFICIENT

The association rate coefficient  $k'_{1\delta}$  applicable to a dissociating excimer ( $D^*$ ) surrounded by an uniform distribution of monomers ( $M$ ) is by definition

$$k'_{1\delta} = -\Gamma_1 - \frac{d \ln S(t)}{dt}, \quad (\text{A1})$$

where  $\Gamma_1$  is the reciprocal of the monomer lifetime and  $S(t)$  is the survival probability of the excited monomer  $M^*$ . With in the independent pair approximation the decay routes of the excited monomer are independent and so<sup>21</sup>

$$S(t) = \exp(-\Gamma_1 t) \left[ 1 - \int_0^t h(u) du \right] \times \exp \left\{ - \int_0^t k_{1\delta}(u) du \right\}, \quad (\text{A2})$$

where  $h(t)dt$  is the probability that the pair of neighboring monomers ( $M^*, M$ ) reform the excimer during a time interval from  $t$  to  $t + dt$  and  $k_{1\delta}(t)$  is given by the Collins–Kimball equation. It relates with  $h(t)dt$  by

$$k_{1\delta} = [M]k_a \left( 1 - \int_0^t h(u) du \right), \quad (\text{A3})$$

as was shown by Noyes.<sup>22</sup> Then, by insertion of Eqs. (A2) and (A3) into Eq. (A1), the association rate coefficient  $k'_{1\delta}$  is obtained as

$$k'_{1\delta} = k_{1\delta} - \frac{d \ln k_{1\delta}}{dt}. \quad (\text{A4})$$

#### APPENDIX B: DERIVATION OF EQ. (38)

The generalized rate coefficient  $k_1$  is defined by the equations

$$\frac{d[M^*]}{dt} = I - \Gamma_1[M^*] + k_2[D^*] - k_1[M^*], \quad (\text{B1})$$

$$\frac{d[D^*]}{dt} = k_1[M^*] - \Gamma_2[D^*] - k_2[D^*]. \quad (\text{B2})$$

The monomer concentration is on the other hand given by

$$[M^*] = I \otimes f_1 + k_2[D^*] \otimes f'_1. \quad (\text{B3})$$

Differentiation of Eq. (B3) yields, after some manipulation,

$$\frac{d[M^*]}{dt} = I - \Gamma_1[M^*] + k_2[D^*] - (I \otimes k_{1\delta} f_1 + k_2[D^*] \otimes k'_{1\delta} f'_1). \quad (\text{B4})$$

Comparison with Eq. (B1) yields

$$k_1 = \frac{I \otimes k_{1\delta} f_1 + k_2[D^*] \otimes k'_{1\delta} f'_1}{I \otimes f_1 + k_2[D^*] \otimes f'_1}. \quad (\text{B5})$$

Equation (B5) can also be obtained in a similar way from the excimer Eq. (B2).



# APPENDIX C: CALCULATION OF THE SECONDARY PRODUCTION RATE

The secondary production rate  $J$ , given by Eq. (20), can be rewritten as

$$J = \mathcal{L}^{-1} \left[ \frac{s + \Gamma_2 + k_2}{s + \Gamma_2 + k_2 (s + \Gamma_1)} \mathcal{L}[f_1] \right] \quad (\text{C1})$$

by use of the identities

$$\mathcal{L}[k_1 f_1] = 1 - (s + \Gamma_1) \mathcal{L}[f_1], \quad (\text{C2})$$

$$\mathcal{L}[k_2 f_2] = \frac{k_2}{s + \Gamma_2 + k_2}. \quad (\text{C3})$$

The Laplace transform of  $f_1$  is numerically computed by means of the change of variable

$$\begin{aligned} \mathcal{L}[f_1] &= \int_0^\infty e^{-st} f_1(t) dt \\ &= \int_0^1 e^{-su/(1-u)} f_1\left(\frac{u}{1-u}\right) \frac{du}{(1-u)^2}. \end{aligned} \quad (\text{C4})$$

The function  $\exp(x^2)\text{erfc}(x)$  was calculated from Das and Periasamy<sup>10(g)</sup> empirical formula, found superior to other analytical approximations.<sup>23</sup>

Calculations of inverse Laplace transforms were made by the Gaver–Stehfest method.<sup>24</sup>

The evaluation of  $J'$  [Eq. (35)] was made following the same procedure.

<sup>1</sup> (a) T. Förster and K. Kasper, *Z. Phys. Chem. N. F.* **1**, 275 (1954); (b) T. Förster and K. Kasper, *Z. Elektrochem.* **59**, 976 (1955).

<sup>2</sup> B. Stevens and E. Hutton, *Nature (London)* **186**, 1045 (1960).

<sup>3</sup> J. B. Birks, *Rep. Prog. Phys.* **38**, 903 (1975).

<sup>4</sup> R. Williams, *J. Chem. Phys.* **28**, 577 (1958).

<sup>5</sup> E. Döller and T. Förster, *Z. Phys. Chem. N. F.* **34**, 132 (1962).

<sup>6</sup> J. B. Birks, D. J. Dyson, and I. H. Munro, *Proc. R. Soc. (London) Ser. A* **275**, 575 (1963).

<sup>7</sup> (a) E. Döller, *Z. Phys. Chem. N. F.* **34**, 151 (1962); (b) J. B. Birks and I. H. Munro, in *Luminescence of Organic and Inorganic Materials*, edited by H. P. Kalmann and G. M. Spruch (Wiley, New York, 1962), p. 230.

<sup>8</sup> M. V. Smoluchowski, *Z. Phys. Chem.* **92**, 129 (1917).

<sup>9</sup> S. A. Rice, in *Comprehensive Chemical Kinetics*, edited by C. H. Bamford, C. F. H. Tipper, and R. G. Compton (Elsevier, New York, 1985).

<sup>10</sup> (a) T. L. Nemzek and W. R. Ware, *J. Chem. Phys.* **62**, 477 (1975); (b) G. S. Beddard, S. Carlin, L. Harris, G. Porter, and C. J. Tredwell, *Photochem. Photobiol.* **27**, 433 (1978); (c) J. C. André, M. Bouchy and W. R. Ware, *Chem. Phys.* **37**, 119 (1979); (d) J. R. Lakowicz, M. L. Johnson, N. Joshi, I. Gryczynski, and G. Laczko, *Chem. Phys. Lett.* **131**, 343 (1986); (e) N. Periasamy, S. Doraiswamy, G. B. Maiya, and B. Vankararaman, *J. Chem. Phys.* **88**, 1638 (1988); (f) D. D. Eads, N. Periasamy, and G. R. Fleming, *J. Chem. Phys.* **90**, 3876 (1989); (g) R. Das and N. Periasamy, *Chem. Phys.* **136**, 361 (1989).

<sup>11</sup> (a) J. M. G. Martinho and M. A. Winnik, *J. Phys. Chem.* **91**, 3640 (1987); (b) J. M. G. Martinho, K. Sienicki, D. Blue, and M. A. Winnik, *J. Am. Chem. Soc.* **110**, 7773 (1988); (c) J. M. G. Martinho, M. Tencer, M. Campos, and M. A. Winnik, *Macromolecules* **22**, 322 (1989).

<sup>12</sup> (a) E. Heumann, *Z. Naturforsch.* **36a**, 1323 (1981); (b) M. H. Hui and W. R. Ware, *J. Am. Chem. Soc.* **98**, 4712 (1976).

<sup>13</sup> S. Lee and M. Karplus, *J. Chem. Phys.* **86**, 1883 (1987).

<sup>14</sup> N. Agmon and A. Szabo, *J. Chem. Phys.* **92**, 5270 (1990).

<sup>15</sup> J. C. André, F. Baros, and M. A. Winnik, *J. Phys. Chem.* **94**, 2942 (1990).

<sup>16</sup> F. C. Collins and G. E. Kimball, *J. Colloid Sci.* **4**, 425 (1949).

<sup>17</sup> M. N. Berberan-Santos and J. M. G. Martinho, *J. Phys. Chem.* **94**, 5847 (1990).

<sup>18</sup> K. Sienicki and M. A. Winnik, *J. Chem. Phys.* **87**, 2766 (1987).

<sup>19</sup> J. Vogelsang and M. Hauser, *J. Phys. Chem.* **94**, 7488 (1990).

<sup>20</sup> M. N. Berberan-Santos and J. M. G. Martinho, *Chem. Phys. Lett.* **178**, 1 (1991).

<sup>21</sup> O. G. Berg, *Chem. Phys.* **31**, 47 (1978).

<sup>22</sup> (a) R. M. Noyes, *J. Chem. Phys.* **22**, 1349 (1954); (b) R. M. Noyes, *Prog. React. Kinet.* **1**, 129 (1961).

<sup>23</sup> J. D. Vedder, *Am. J. Phys.* **55**, 762 (1987).

<sup>24</sup> (a) D. P. Gaver, *Oper. Res.* **14**, 444 (1966); (b) H. Stehfest, *Comm. ACM* **13**, 47, 624 (1970).